

## Research Article

# Preparation and Characterization of Printed LTCC Substrates for Microwave Devices

Yanfeng Shi <sup>1,2</sup>, Yongqiang Chai <sup>1,2</sup> and Shengbo Hu <sup>1,2</sup>

<sup>1</sup>Institute of Intelligent Information Processing, Guizhou Normal University, Guiyang 550001, China

<sup>2</sup>Department of Education, Center for RFID and WSN Engineering, Guizhou, Guiyang 550001, China

Correspondence should be addressed to Shengbo Hu; [hsb@nssc.ac.cn](mailto:hsb@nssc.ac.cn)

Received 3 December 2018; Revised 13 February 2019; Accepted 21 February 2019; Published 1 April 2019

Academic Editor: Gerard Ghibaudo

Copyright © 2019 Yanfeng Shi et al. This is an open access article distributed under the Creative Commons Attribution License, which permits unrestricted use, distribution, and reproduction in any medium, provided the original work is properly cited.

A novel LTCC substrate manufacturing process based on 3D printing was investigated in this paper. Borosilicate glass-alumina substrates with controlled size and thickness were successfully manufactured using a self-developed dual-nozzle hybrid printing system. The printing parameters were carefully analyzed. The mechanical and dielectric properties of the printed substrate were examined. The results show that the printed substrates obtain smooth surface ( $Ra=0.92\ \mu\text{m}$ ), compact microstructure (relative density 93.7%), proper bending strength (156 mPa), and low dielectric constant and loss ( $\epsilon_r=6.2$ ,  $1/\tan\delta=0.0055$ , at 3 GHz). All of those qualify the printed glass-ceramic substrates to be used as potential LTCC substrates in the microwave applications. The proposed method could simplify the traditional LTCC technology.

## 1. Introduction

The rapid development of high frequency wireless communication has resulted in an increasing demand for miniaturized, high integration, and multi-functional microwave ceramic devices. It also puts forward the requirement of electronic packaging technology. Low temperature co-fired ceramic (LTCC) technology provides a good solution for the miniaturization and lightweight of electronic components and modules in high frequency applications. As one of the functional parts of LTCC devices, LTCC substrate materials have been extensively investigated in the past decades [1–6], and many materials have been developed in the form of glass-ceramic or glass/ceramic according to the needs of the specific applications. One of the most important processes in LTCC substrate manufacturing is tape casting, which includes procedures like slurry preparation, mixing, degassing, casting, drying, punching, etc. Although high-quality ceramic substrate can be obtained, the traditional tape casting process is so complex and low precision that not only affects the performance of microwave devices, but also is difficult to adapt to the trend of rapid, integrated, small batch in device production. And the tape casting process has brought a lot of environmental pollution. To solve these

problems, many scholars have carried out new researches on materials and technologies [7, 8].

Three-dimensional printing (3DP), known as additive manufacturing, has become the focus of media and public attention in recent years as the decades-old technology has at last approached the performance necessary for direct production of end-use devices [9]. J.J. Adams et al. [10] reported a new 3DP technique which enables the integration of an antenna directly onto the package of a small wireless sensor node that ensures near-optimal bandwidth performance of the small antenna. Kong et al. [11] reported a five-layer fully 3D-printed quantum-dot-based light-emitting diodes (QD-LEDs), showing the ability to rapidly print electronic devices with embedded circuitry that would enable myriad applications [12]. Therefore, the rising interest in 3DP technology is resulting in rethinking of traditional approaches for the design and manufacture of multi-layered LTCC devices.

In this paper, we report a novel LTCC substrate manufacturing process based on 3D printing. The glass-ceramic substrates were printed using a dual-nozzle hybrid printing system. The printing parameters were carefully discussed. The density, microstructure, mechanical strength, and dielectric properties of the printed substrate were investigated.

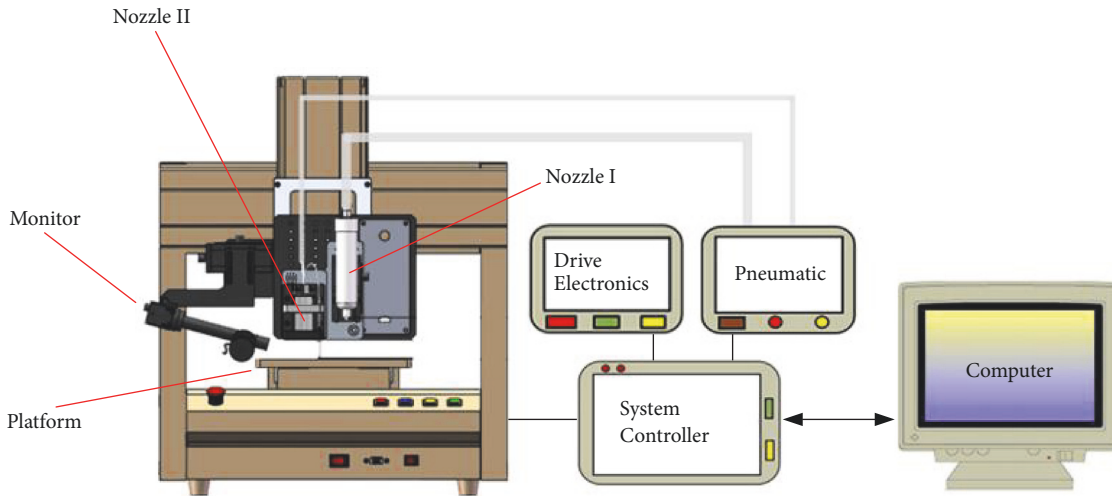


FIGURE 1: Schematic of dual-nozzle hybrid printing system.

## 2. Experimental

**2.1. Materials.** A typical glass-ceramic system, borosilicate glass-alumina was used in this work. Commercially available borosilicate glass and high purity  $\text{Al}_2\text{O}_3$  powders were both purchased from Sinopharm Chemical Reagent Co., Ltd. The main composition of the obtained glass is 16.5wt % CaO, 14.5wt %  $\text{Al}_2\text{O}_3$ , 8.9wt %  $\text{B}_2\text{O}_3$ , 54wt %  $\text{SiO}_2$ , and 4.4wt % MgO. Both of the powders were ball-milled with alumina balls in ethanol for 24 h. The average diameters ( $D_{50}$ ) of the resulting powders were  $1.56 \mu\text{m}$  for glass and  $0.98 \mu\text{m}$  for  $\text{Al}_2\text{O}_3$  as measured by laser particle analyzer (Rise 2028, Jinan Rise Co., Ltd, China).

**2.2. Slurry Preparation.** The glass-ceramic slurry (40wt %) was prepared in a ball mill for 4 h to ensure good dispersion and consistency, using deionized water as solvent. The mass ratio of glass and ceramic powders was 60:40 (glass:  $\text{Al}_2\text{O}_3$ ). Darvan C (R.T. Vanderbilt Co., Norwalk, CT), a 30wt % ammonium polyacrylate solution, was used as dispersant and hydroxyethyl cellulose (Aladdin Industrial Co., Shanghai, China) as viscosifying agent. Polyethylene glycol (Sinopharm Chemical Reagent, Shanghai, China) was added as humectant. Antifoaming agent (Aladdin Industrial Co., Shanghai, China) was also added to prevent foaming, and ammonia water was used to adjust the PH value.

**2.3. Fabrication of LTCC Substrates.** In order to achieve the integrated manufacturing of functional devices, we designed and installed a dual-nozzle hybrid printing system, as shown in Figure 1. The Nozzle I of the printing system adopts direct writing method, using an air pressure-assisted syringe, for high viscosity materials printing. Nozzle II uses piezoelectric jetting system for high precision printing of low viscosity functional materials. The glass-ceramic LTCC substrates were printed by nozzle I. The synthetic motion of platform and nozzle was driven control system. The pre-prepared glass-ceramic slurry was extruded from the nozzle under a certain

pressure and deposited on the platform and formed the desired layer shape. Of course, multilayer devices could be constructed layer by layer with a nozzle elevation repeatedly. The substrate shape was controlled by the path of nozzle movement, which could be achieved by programming with G code. During the printing experiment, the inner diameter of the nozzle used was 0.16 mm, the moving speed of X-Y direction was 300 mm/s, and the air pressure was 150 kPa. Tubular specimens were also fabricated with the inner diameter of 3 mm, the outer diameter of 7 mm, and the height of 10 mm for dielectric properties test. Samples were debinded at  $450^\circ\text{C}$ , then sintered at  $800\text{-}900^\circ\text{C}$  in the air for 2 hours, and then cooled in a furnace.

**2.4. Characterization.** The relative density of the sintered substrate was measured by Archimedes method. The mechanical strength of glass-ceramic was investigated by a universal testing machine (WDW2000, Haerbin Kexin ins., China) using three-point bending test method. The roughness of upper surface of printed substrate was measured by a probe instrument (JB-4C, Shanghai Optical Instrument Co., China). The microstructure was observed by the scanning electron microscope (Phenom Pro, Phenom, Netherlands). The dielectric properties were measured by vector network analyzer (AV36580A, 41st Institute of CETC, China).

## 3. Results and Discussion

Figure 2 shows the printed LTCC substrates, tubular specimen, and their surface roughness. LTCC substrates with dimensions of  $10 \times 10$  mm,  $5 \times 5$  mm, and  $10 \times 5$  mm are obtained as designed (Figure 2(a)), with smooth and flat surface. The printed tubular specimen for dielectric testing is shown in Figure 2(b). The thickness of the substrate is  $105 \pm 5 \mu\text{m}$ . The average roughness of the upper surface is  $0.92 \mu\text{m}$  as shown in Figure 2(c). Figure 3 shows the SEM images of upper and cross section of sintered substrate. It can be seen that the sintered glass-ceramic substrate achieves compact

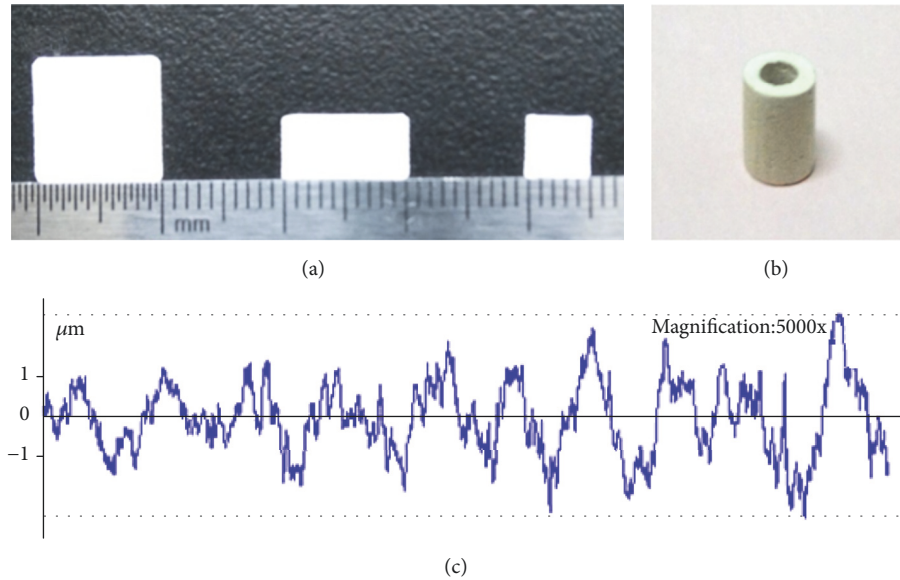


FIGURE 2: Printed LTCC samples and its roughness. (a) Substrates with different size. (b) Printed tubular specimen for dielectric testing. (c) Roughness of printed substrate.

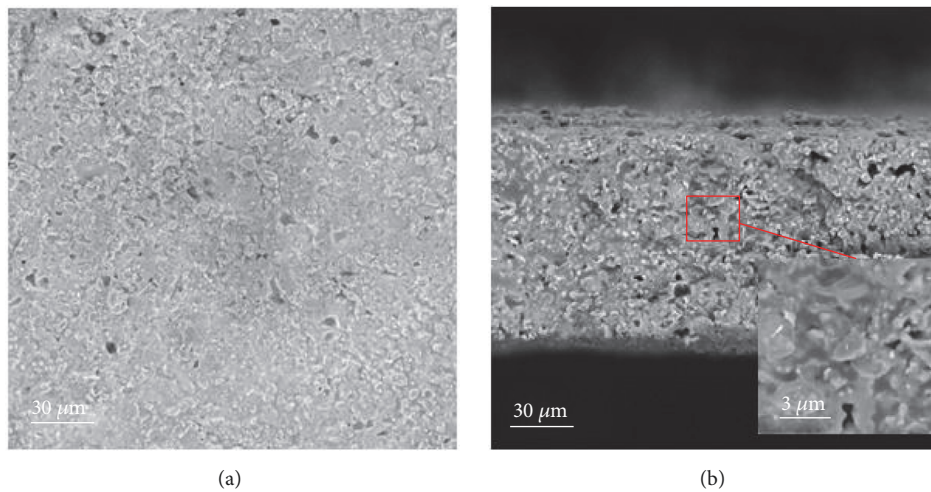


FIGURE 3: SEM images of printed substrate. (a) The upper surface. (b) The cross-sectional view.

structure with fewer pores, as the glass melts and encapsulates the ceramic phase under high-temperature sintering.

It is clear that substrate printing is a process of slurry deposition and fusion. The printing quality depends on the properties of slurry, the model design, and the match of printing parameters. Viscosity of slurry is an important factor that affects the substrate printing. If the viscosity is too high, the extruded rod-like materials may not be fused together and forms fluctuant surface. If it is too low, the slurry cannot print and maintain the desired shape. At the same time, lower viscosity of slurry will also slow down the drying process, resulting in the size deviation and uneven thickness of printed substrate. The experimental results indicate that the slurry with the viscosity about 2000-5000 mPa·s can be extruded continuously and uniformly.

The printing parameters include the nozzle diameter ( $d_n$ ), pressure ( $p$ ), platform moving velocity ( $v_p$ ), the gap between the nozzle and the platform ( $h$ ), etc., which greatly affect the controllable printing of glass-ceramic substrate. The surface roughness ( $Ra$ ) and thickness of the substrate are mainly related to  $d_n$  and  $h$ . The smaller the nozzle diameter  $d_n$  used, the easier the smooth and thin substrate to be obtained. The value of  $h$  should be carefully considered according to  $d_n$  and properties of slurry. If  $h$  is too high, the deposition of the slurry will not be accurate. If it is too low, many traces appear on the surface because of the agitation of the nozzle. The continuous and stable printing process also requires the match of  $v_p$  and air pressure  $p$ , as  $p$  determines the outlet velocity of slurry ( $v_s$ ). In general, we need to ensure that  $v_p$  is equal to  $v_s$  for stable printing, and their speed should

TABLE 1: Properties of printed glass-ceramic substrate.

Properties	This work	DuPont
Composition	60 %BSG+40 %alumina	951
Sintering temperature (°C)	875	-
Relative Density (%)	93.7	-
Dielectric constant, $\epsilon_r$ (3 GHz)	6.2	7.8
Dielectric loss, $1/\tan \delta$ (3 GHz)	0.0055	0.006
Bending strength (mPa)	156	-

not be too fast. It is assumed that the flow of slurry in the nozzle is a laminar flow, and the slurry is an incompressible uniform fluid with constant physical parameters. Based on the motion analysis of slurry during extrusion, we can deduce the relationship between  $v_p$  and  $p$  as follows:

$$v_p = \frac{\Delta p + \rho g L}{2\mu L} \cdot \frac{R^4}{d_n^2} \quad (1)$$

where  $\Delta p = p - p_2$ ,  $p$  is the pressure applied on the slurry,  $p_2$  is atmospheric pressure,  $\rho$  is the density of fluid fills in the syringe,  $L$  is the height of fluid fills in the syringe,  $\mu$  is the viscosity of slurry,  $R$  is the radius of syringe, and  $d_n$  is the diameter of nozzle.

As a result, borosilicate glass-alumina LTCC substrate with controlled size and smooth surface was obtained. It was comparable to commercial substrates, such as DuPont 951 [3].

The ideal LTCC substrate materials should possess several characteristics such as low dielectric constant (below 10) and low dielectric loss, high thermal conductivity, robustness against environmental stress, and low cost [5]. Table 1 shows the physical and dielectric properties of the printed borosilicate glass-alumina substrate in this study and the comparison with Dupont 951 [3]. The relative density of the LTCC substrate reaches 93.7 % after being sintered at 875 °C for 2 hours, and the average bending strength is 156 mPa. The dielectric constant  $\epsilon_r$  at 3 GHz is 6.2 and the loss  $1/\tan \delta$  is 0.0055. The value of  $\epsilon_r$  is smaller than that of calculated by the equation derived by Penn et al. [6]. The reduction of  $\epsilon_r$  can be attributed to the relative density of ceramic-glass composites. As can be seen from Figure 3(b), there are some micro-pores still existing in the substrate that can reduce the dielectric constant of the material effectively. The pores in the substrate also led to lower dielectric loss and lower bending strength. Hence, the observed properties indicate that the printed glass-ceramic substrate can be a possible candidate for LTCC substrate applications.

#### 4. Conclusion

A novel method to prepare LTCC substrate based on 3D printing was proposed and preliminarily studied. A dual-nozzle hybrid printing system was developed for this purpose. Borosilicate glass-alumina LTCC substrates with controlled size and thickness were successfully manufactured in this work. To achieve high quality printing, the viscosity of slurry was carefully tailored to 2000-5000 mPa·s; the printing parameters should also be optimized accordingly.

The printed substrates are characterized with smooth surface ( $Ra=0.92 \mu\text{m}$ ), low dielectric constant and loss ( $\epsilon_r=6.2$ ,  $1/\tan \delta=0.0055$ , at 3 GHz), and proper mechanical strength (156 mPa), which indicates the great potential for microwave applications. In all, this method could simplify the traditional LTCC technology and further experiment on integrated printing of devices is in progress.

#### Data Availability

The data generated or analyzed during this study are included within the article, but the programs analyzed during the current study are not publicly available as they are part of the simulation programs in use.

#### Conflicts of Interest

The authors declare that there are no conflicts of interest regarding the publication of this paper.

#### Acknowledgments

This research is supported by the National Natural Science Foundation of China (Grant no. 61561009), the Innovation Group Project, Department of Education, Guizhou (Grant no. [2017]031), the Guizhou Science and Technology Foundation (Grant no. LKS [2013] 25), and the Guizhou Science and Technology Foundation (Grant no. [2014] 7036). The authors appreciate the help from Guizhou Aerospace Institute of Measuring and Testing Technology for mechanical and dielectric tests.

#### References

- [1] Q.-L. Zhang, H. Yang, and H.-P. Sun, "A new microwave ceramic with low-permittivity for LTCC applications," *Journal of the European Ceramic Society*, vol. 28, no. 3, pp. 605–609, 2008.
- [2] M. Sobocinski, M. Teirikangas, J. Peräntie et al., "Decreasing the relative permittivity of LTCC by porosification with poly(methyl methacrylate) microspheres," *Ceramics International*, vol. 41, pp. 10871–10877, 2015.
- [3] DuPont, "DuPont green tape 951 low temperature ceramic system," *Technical Data Sheet*, 2011.
- [4] N. Mori, Y. Sugimoto, J. Harada, and Y. Higuchi, "Dielectric properties of new glass-ceramics for LTCC applied to microwave or millimeter-wave frequencies," *Journal of the European Ceramic Society*, vol. 26, no. 10-11, pp. 1925–1928, 2006.
- [5] C.-C. Chiang, S.-F. Wang, Y.-R. Wang, and W.-C. J. Wei, "Densification and microwave dielectric properties of CaO-B2O3-SiO2 system glass-ceramics," *Ceramics International*, vol. 34, no. 3, pp. 599–604, 2008.
- [6] S. J. Penn, N. M. Alford, A. Templeton et al., "Effect of porosity and grain size on the microwave dielectric properties of sintered alumina," *Journal of the American Ceramic Society*, vol. 80, no. 7, pp. 1885–1888, 1997.
- [7] H. Amorín, I. Santacruz, J. Holc et al., "Tape-casting performance of ethanol slurries for the processing of textured PMN-PT ceramics from nanocrystalline powder," *Journal of the American Ceramic Society*, vol. 92, no. 5, pp. 996–1001, 2009.

- [8] A. Şakar-DeliormanI, E. Çelik, and M. Polat, “Thermal analysis and microstructural characterization of ceramic green tapes prepared by aqueous tape casting,” *Journal of Thermal Analysis and Calorimetry*, vol. 94, no. 3, pp. 663–667, 2008.
- [9] E. MacDonald and R. Wicker, “Multiprocess 3D printing for increasing component functionality,” *Science*, vol. 353, no. 6307, Article ID aaf2093, 2016.
- [10] J. J. Adams, S. C. Slimmer, J. A. Lewis, and J. T. Bernhard, “3D-printed spherical dipole antenna integrated on small RF node,” *IEEE Electronics Letters*, vol. 51, no. 9, pp. 661-662, 2015.
- [11] Y. L. Kong, I. A. Tamargo, H. Kim et al., “3D printed quantum dot light-emitting diodes,” *Nano Letters*, vol. 14, no. 12, pp. 7017–7023, 2014.
- [12] J. A. Lewis and B. Y. Ahn, “Device fabrication: Three-dimensional printed electronics,” *Nature*, vol. 518, no. 7537, pp. 42-43, 2015.



**Hindawi**

Submit your manuscripts at  
[www.hindawi.com](http://www.hindawi.com)

